The Foundations of a Unified Approach to Mathematical Modelling of Angiogenesis

Matthew E. Hubbard
School of Computing
University of Leeds,
Leeds, UK

Pamela F. Jones
Leeds Institute of Molecular Medicine,
University of Leeds,
Section of Molecular Gastroenterology,
Wellcome Trust Brenner Building,
St. James's University Hospital,
Leeds, U.K
and
Brian. D. Sleeman
School of Mathematics,
University of Leeds,
Leeds, UK.

1 Introduction to Angiogenesis

It is a well known fact that tumours can grow to approximately 1-2mm^3 before their metabolic demands are impeded due to the diffusion limit of oxygen and nutrients. In order to grow beyond this size, the tumour switches to an angiogenic phenotype and induces the sprouting of new blood vessels from the surrounding stroma. Angiogenesis is a highly controlled process,

normally regulated by a fine balance of pro- and anti-angiogenic factors and the switch to a pro-angiogenic state is a prerequisite for further outgrowth of the tumour [5]. In addition to sprouting capillaries, neovasculature can also arise in tumours through other mechanisms including intussusceptive angiogenesis, [2], the recruitment of endothelial progenitor cells, [13], vessel co-option [16] and vasculogenic mimicry [7].

Sprouting angiogenesis [15] is the most widely studied mechanism for neovascular growth from the mathematical point of view and the one to which we shall apply the unifying ideas presented in this paper. The additional mechanisms mentioned above depend in a fundamental way on those exploited in sprouting angiogenesis and it is suggested that the modelling ideas used in this paper are amenable to these wider aspects of tumour angiogenesis. Angiogenesis also arises in many physiological situations including embryonic development, wound healing and reproduction [9]. It also plays a basic role in certain pathologies such as diabetes, rheumatoid arthritis, cardiovascular ischemic complications and cancer [8]. In cancer, sprouting angiogenesis is not only important in primary tumours, it is also involved in metastasis formation and subsequent growth. Hence, the modelling ideas presented here are applicable to a wide range of pathological conditions.

Angiogenesis involves a series of orchestrated steps, reviewed in [25, 21]. A pro-angiogenic signal, such as Vascular Endothelial Growth Factor (VEGF), activates the normally quiescent endothelial cells, which results in a number of biochemical/cellular responses [6]. One response is the secretion of activated proteases, which locally degrade the extracellular matrix and basement membrane. This allows the endothelial cells to invade the surrounding matrix and subsequently proliferate and migrate, usually moving by chemotaxis towards the source of the growth factor, as shown in Figure 1.

Further exposure to pro-angiogenic signalling leads to differentiation and polarization of the migrating endothelial cells, which subsequently form a tubule with a lumen. In order to form a functional vessel, a loop has to form: the tips of two adjacent tubules coalesce to form an anastomosis through which blood can begin to flow. The stabilization of these new, immature blood vessels is achieved by the recruitment of mural cells, pericytes and the generation of extracellular matrix, see Figure 2.

Tumour angiogenesis occurs by the same mechanisms, with many tumour cells themselves secreting the pro-angiogenic factor (usually VEGF) needed to induce new vessel growth [12]. The architecture of tumour vessels is often leaky [10], caused by fewer EC-EC contacts, resulting in different transport

properties for the movement of fluid and proteins from blood to the tumour tissue. These differences can be subsequently modelled in modifications of the premise.

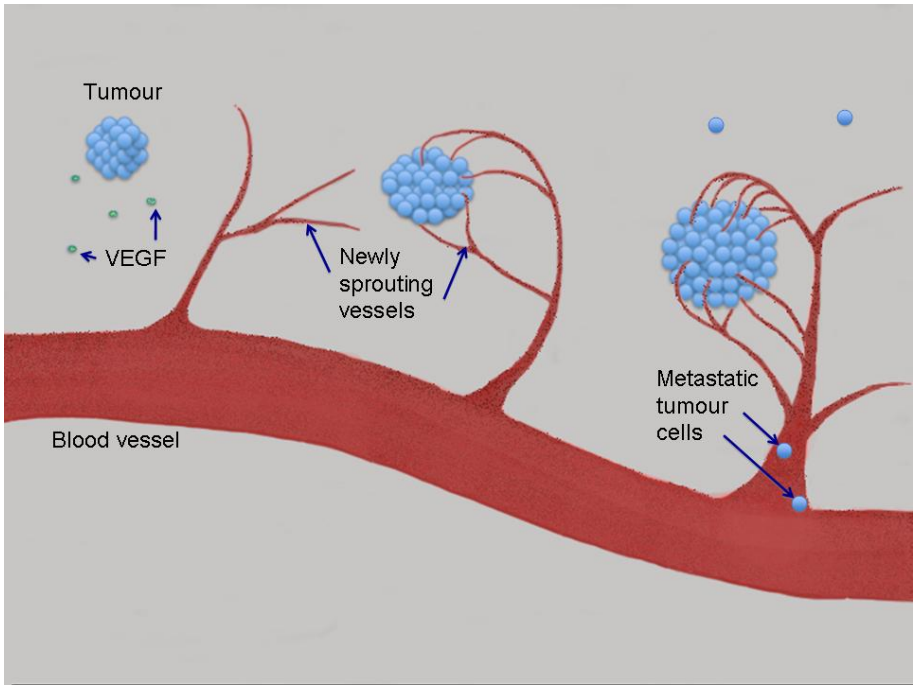

Figure 1: Endothelial cell migration towards a tumour source of VEGF and the formation of a neovascular network leading to metastasis.

Mathematical modelling of sprouting angiogenesis has been under intensive investigation over the past two decades and has been approached from several points of view. Among the earliest modelling ideas was that used by Stokes and Lauffenberger [28] who formulated the movement of endothelial cells in terms of stochastic differential equations. Simulations carried out in [28] corresponded very well with the neovascular structures observed in *in vitro* experiments. However the models did not include some of the important players in angiogenesis; particularly the role of fibronectin degradation and haptotaxis. Somewhat later Chaplain and Stuart [4] and Anderson and Chaplain [3] used the idea of conservation of mass to derive a nonlinear partial differential equation governing the evolution of endothelial cell density. This model included chemotaxis of VEGF and haptotaxis of fibronectin. Simulations of vascular networks were carried out by using a

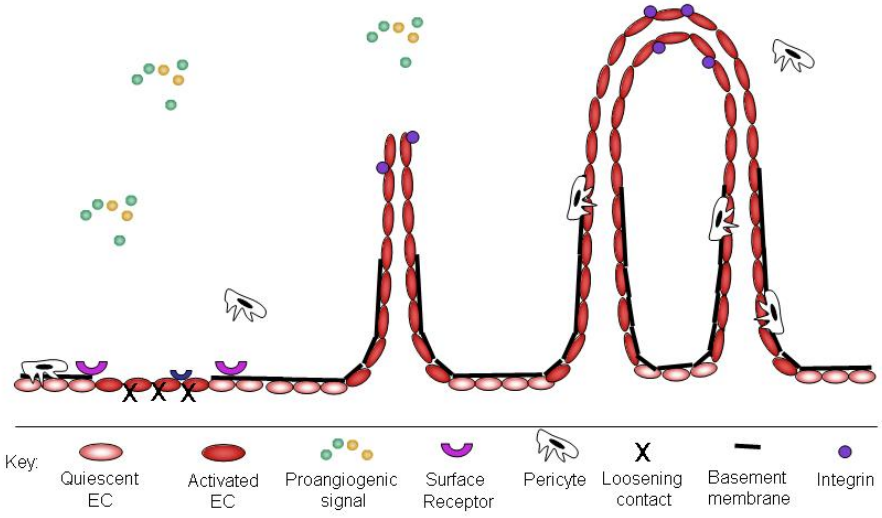

Figure 2: The recruitment of mural cells and pericytes leading to stabilisation of immature blood vessels and formation of anastomosis.

numerical discretisation of the PDE resulting in a pseudo master equation from which certain terms were considered to be akin to transition probability functions. The resulting networks generated by this approach correlated well with *in vitro* experimental observations. In [18, 19] Levine et al. were the first to develop an individual cell-based model formulated in terms of the theory of reinforced random walks. This model is expressed in terms of a master equation and identifies certain transition probability functions which can depend on a variety of growth promoters and growth inhibitors including VEGF, fibronectin and proteolytic enzymes. Simulations with this model give excellent agreement with results of *in vitro* experiments.

In view of the relative merits of each of the above mathematical modelling approaches to sprouting angiogenesis it is of considerable interest to investigate an underlying theme which unifies these modelling techniques. In this paper we demonstrate that a basic formulation in terms of stochastic differential equations provides such a unification. Furthermore the ideas expressed here can be used to analyse and validate models of intussusceptive angiogenesis, vessel co-option, vasculogenic mimicry and lymphangiogenesis.

The plan of this paper is as follows; in section 2 we introduce the fundamental stochastic differential equation and draw out its connection with the Fokker-Planck equation. We then review, in this setting, the pioneering work of Stokes and Lauffenberger [28]. Section 3 is concerned with the master equation and its connection to the Fokker-Planck equation. This leads naturally to the cell-based models of Levine et al. [18, 19]. In section 4 we consider the formulation of cell density models based on the conservation of mass hypothesis. These models are essentially expressed in terms of Fokker-Planck equations which in turn are intimately related to the stochastic differential equation. Section 5 describes angiogenesis modelling directly from the stochastic differential equation and illustrates the ideas with some preliminary stochastic simulations. The paper concludes in section 6 with an indication of future research together with some open problems.

2 Multivariable Stochastic Differential Equations and the Fokker-Planck Equation

Let $\mathbf{x}(t)$ be an n-dimensional vector representing the co-ordinates of the position of a particular endothelial cell at time t. We begin by supposing

that $\mathbf{x}$ is governed by a system of stochastic differential equations of the form

$$d\mathbf{x} = \mathbf{A}(\mathbf{x}, t)dt + \mathbf{B}(\mathbf{x}, t)d\mathbf{W}(t), \tag{2.1}$$

where $\mathbf{A}(\mathbf{x}, t)$ is an $n \times 1$ vector drift coefficient, $\mathbf{B}(\mathbf{x}, t)$ is an $n \times n$ matrix of diffusion coefficients and $d\mathbf{W}(t)$ is an n-variable Wiener process.

Equation (2.1) is a very general form of a stochastic differential system. In the context of angiogenesis the drift coefficient $\mathbf{A}(\mathbf{x}, t)$ is to be thought of as the taxis, including chemotaxis as well as haptotaxis, of an EC in response to growth factors, growth inhibitors as well as anti-angiogenic therapies. The diffusion coefficient $\mathbf{B}(\mathbf{x}, t)$ can also be quite general and as well as possibly dependent on growth factors and growth inhibitors can also be modelled to account for heterogeneity of the substrate tissue.

To describe the Wiener process we limit the discussion to the one-variable case. To begin with we introduce the idea of a conditional probability density function;

Definition 1

The quantity $p(x, t|x_0, t_0)$ is called the conditional probability density function and is the probability of being in state x at time t after previously being in state x_0 at time t_0.

For the purposes of the theory developed here we assume random Brownian motion, in which case $p(x, t|x_0, t_0)$ represents a Gaussian. That is

$$p(x, t|x_0, t_0) = [2\pi(t - t_0)]^{-1/2} exp[-(x - x_0)^2/2(t - t_0)],$$

The Wiener process is then Gaussian with mean value

$$\langle W(t)\rangle \equiv \int_{-\infty}^{\infty} xp(x, t|x_0, t_0)dx = x_0 \tag{2.2}$$

and variance

$$\langle [W(t) - x_0]^2\rangle = t - t_0. \tag{2.3}$$

For the multivariate Wiener process we define

$$\mathbf{W}(t) = [W_1(t), W_2(t), \ldots, W_n(t)]\,. \tag{2.4}$$

It is common practice to refer to $W(t)$ as *white* noise.

Remark 1 In the formulation of the theory the definition of $\mathbf{x}$ can be extended to include growth factors and growth inhibitors.

Remark 2 The formulation of angiogenesis through the stochastic differential equation (2.1) is the key modelling tool used by Stokes and Lauffenberger [28, 29] discussed below.

It is a remarkable fact that there is a direct equivalence between the stochastic equation (2.1) and a Fokker-Planck equation governing the probability density $p(\mathbf{x}, t|\mathbf{x}_0, t_0)$ associated with the stochastic process. To see this we again consider the one variable case and make use of the Itô calculus and in particular Itô's formula [11]. Suppose $x(t)$ is governed by the stochastic differential equation;

$$dx(t) = a[x(t), t]dt + b[x(t), t]dW(t), \tag{2.5}$$

then using Itô's formula [11], p95, we have

$$\begin{aligned} \langle df[x(t)]\rangle/dt &= \langle \frac{df[x(t)]}{dt}\rangle = \frac{d}{dt}\langle f[x(t)]\rangle \\ &= \langle a[x(t), t]\partial_x f + \frac{1}{2}b[x(t)]^2\partial_x^2 f\rangle \,. \end{aligned}$$

If $x(t)$ has a conditional probability density $p(x, t|x_0, t_0)$ then

$$\begin{aligned} \frac{d}{dt}\langle df[x(t)]\rangle &= \int dx f(x)\partial_t p(x, t|x_0, t_0), \\ &= \int dx[a(x, t)\partial_x f + \frac{1}{2}b(x, t)^2\partial_x^2 f]p(x, t|x_0, t_0). \end{aligned}$$

After an integration by parts we get

$$\int dx f(x)\partial_t p = \int dx f(x)\{-\partial_x[a(x, t)p] + \frac{1}{2}\partial_x^2[b(x, t)^2 p]\}$$

and since $f(x)$ is arbitrary we obtain

$$\partial_t p = -\partial_x[a(x, t)p] + \frac{1}{2}\partial_x^2[b(x, t)^2 p], \tag{2.6}$$

which is a Fokker-Planck equation for $p(x, t|x_0, t_0)$.

If we argue in the same way for the stochastic differential equation system (2.1) we obtain the equation

$$\partial_t p = -\sum_i \partial_i \left[A_i(\mathbf{x}, t)p\right] + \frac{1}{2}\sum_{i,j}\partial_i\partial_j\{\left[\mathbf{B}(\mathbf{x}, t)\mathbf{B}^T(\mathbf{x}, t)\right]_{ij} p\}, \tag{2.7}$$

where T denotes transpose. Equation (2.7) is the Fokker-Planck equivalent of the stochastic system (2.1).

We now relate the equations (2.1) and (2.7) to the modelling ideas of Stokes and Lauffenberger [28]. There, the principal modelling components are, the tip velocity, $\mathbf{v}$, position, $\mathbf{x}$, and the cell density, ρ, within each capillary sprout. The stochastic ordinary differential equation governing the velocity, $\mathbf{v}_i$, of the tip cell of the i^{th} sprout is assumed to be;

$$d\mathbf{v}_i = -\beta \mathbf{v}_i(t)dt + \sqrt{\alpha} d\mathbf{W}_i(t) + \kappa \nabla a \sin|\frac{\phi_i}{2}|dt. \tag{2.8}$$

From equation (2.7) the associated probability density function is governed by the Fokker-Planck equation

$$\partial_t p = \beta \sum_i \partial_i p - \kappa \nabla \cdot (\sin|\frac{\phi_i}{2}| p \, \nabla a) + \frac{\alpha}{2} \Delta p. \tag{2.9}$$

The angle ϕ_i is defined as follows;

$$\cos\phi_i = \left[\frac{(x_a - x_i)\cos\theta_i + (y_a - y_i)\sin\theta_i}{((x_a - x_i)^2 + (y_a - y_i)^2)^{1/2}} \right], \tag{2.10}$$

and is the angle between the direction the tip cell of the i^{th} sprout is moving and that towards the chemo-attractant source situated at (x_a, y_a). The angle θ_i is the direction of cell movement measured relative to the x-axis.

Cells within a sprout are measured in terms of an average cell density, ρ, and constrained by two densities, ρ_{min} and ρ_{max}. The density ρ_{min} corresponds to the lowest density required to maintain a contiguous vessel while ρ_{max} is the confluent density at which the micro-endothelial cell stops growing as observed both *in vivo* and *in vitro*. Stokes and Lauffenberger [28] postulate that if a sprout's density falls to ρ_{min} then the sprout cannot further elongate and new buds cannot start growing off it. Consequently if the proliferation rate and cell redistribution rate are not great enough in comparison with the migration rate, the vessel will not be able to elongate because additional cells will not be available to maintain a contiguous vessel. At ρ_{max} cells in this sprout stop proliferating.

Branches bud off existing sprouts and loops with a probability density, p_b, the probability per unit time per unit length of vessel. It is assumed constant for all vessels and all positions and times. No branches or loops can start growing off a sprout or loop whose density is ρ_{min}. Anastomosis, the

formation of closed loops, occurs whenever a sprout tip runs into another sprout or loop. When this happens the tip dies and only ρ is continually calculated. Finally the rate of change of cell density is modelled to depend on, the proliferation rate of cells in the sprout, the rate at which the sprout is elongating, the redistribution of cells from the parent vessel to sprout i and the redistribution of cells from sprout i to sprouts j growing off of sprout i. For the relevant modelling equation see [28] equation (9).

The simulations carried out by Stokes and Lauffenberger [28] on their model give quite realistic neovascular structures. However their model only considers the chemotactic response of endothelial cells to VEGF and does not include other important growth factors and growth inhibitors or the haptotactic response to fibronectin. These can, in principle, be incorporated into the model but here we wish to view the Stokes and Lauffenberger model in the wider context of individual cell-based models formulated on the idea of reinforced random walks as discussed below.

3 Master Equations and the Fokker-Planck Equation

The individual cell-based models of angiogenesis developed by Levine et al. [18, 19] and Plank and Sleeman [23] are based on the theory of reinforced random walks in which the fundamental ingredient is the concept of a master equation. To begin with we introduce the concept of a transition probability $W(\mathbf{x}|\mathbf{x}_0, t)$ related to the conditional probability density $p(\mathbf{x}, t|\mathbf{x}_0, t_0)$ via the following:

$$i) \lim_{\triangle t \to 0} p(\mathbf{x}, t + \triangle t|\mathbf{x}_0, t)/\triangle t = W(\mathbf{x}|\mathbf{x}_0, t) \tag{3.1}$$

uniformly in $\mathbf{x},\ \mathbf{x}_0$ and t for $\mid \mathbf{x} - \mathbf{x}_0 \mid \geq \epsilon$ and all $\epsilon > 0$;

$$ii) \lim_{\triangle t \to 0} \frac{1}{\triangle t} \int_{|\mathbf{x}-\mathbf{x}_0|<\epsilon} d\mathbf{x}(x_i - x_{0i}) p(\mathbf{x}, t + \triangle t|\mathbf{x}_0, t) = A_i(\mathbf{x}_0, t) + O(\epsilon); \tag{3.2}$$

$$iii) \lim_{\triangle t \to 0} \frac{1}{\triangle t} \int_{|\mathbf{x}-\mathbf{x}_0|<\epsilon} d\mathbf{x}(x_i - x_{0i})(x_j - x_{0j}) p(\mathbf{x}, t + \triangle t|\mathbf{x}_0, t) = B_{ij}(\mathbf{x}_0, t) + O(\epsilon); \tag{3.3}$$

the last two being uniform in $\mathbf{x}_0,\ \epsilon$ and t.

In addition the quantity $A_i(\mathbf{x}_0, t)$ is to be identified with the i^{th} component of the drift coefficient $\mathbf{A}(\mathbf{x}_0, t)$ while the quantity $B_{ij}(\mathbf{x}_0, t)$ is to be identified with the ij^{th} component of the diffusion matrix $\mathbf{B}(\mathbf{x}_0, t)\mathbf{B}^T(\mathbf{x}_0, t)$.

Following Gardiner [11], p52, the *Master Equation*, in the case of jump processes, is defined as

$$\partial_t p(\mathbf{z}, t|\mathbf{y}, t') = \int d\mathbf{x} \left[W(\mathbf{z}|\mathbf{x}, t) p(\mathbf{x}, t|\mathbf{y}, t') - W(\mathbf{x}|\mathbf{z}, t) p(\mathbf{z}, t|\mathbf{y}, t') \right]. \quad (3.4)$$

In the situation when the state space consists only of integers, as required in our individual cell-based models, the *master equation* takes the form

$$\partial_t P(\mathbf{n}, t|\mathbf{n}', t') = \sum_{\mathbf{m}} \left[W(\mathbf{n}|\mathbf{m}, t) P(\mathbf{m}, t|\mathbf{n}', t') - W(\mathbf{m}|\mathbf{n}, t) P(\mathbf{n}, t|\mathbf{n}', t') \right]. \quad (3.5)$$

For simplicity we again consider the one-dimensional case. Suppose the transition probability $W(n|n', t)$ is given by the form

$$W(n|n', t) = \hat{\tau}^+(n')\delta_{n,n'+1} + \hat{\tau}^-(n')\delta_{n,n'-1} \quad (3.6)$$

where $\delta_{m,n}$ is the Kronecker delta function, $\hat{\tau}^+(n)$ is the transition probability of a one-step jump from n to $n+1$ while $\hat{\tau}^-(n)$ is the transition probability of a one-step jump from n to $n-1$. Then the master equation (3.5) takes the form

$$\begin{aligned} \partial_t P(n, t|n', t') &= \hat{\tau}^+(n-1)P(n-1, t|n', t') + \hat{\tau}^-(n+1)P(n+1, t|n', t') \\ &\quad -[\hat{\tau}^+(n) + \hat{\tau}^-(n)]P(n, t|n', t'). \end{aligned} \quad (3.7)$$

This form of the master equation is, except for a slight notational change, precisely the master equation we have exploited in previous work on cell-based modelling of angiogenesis to describe EC motion. In this connection we cite the references [18, 19], [23], [27]and [24].

In higher dimensions the master equation takes the form

$$\begin{aligned} \partial_t P(\mathbf{n}, t) &= \sum_N \{ [\hat{\tau}_N^-(\mathbf{n} + \mathbf{r}^N)P(\mathbf{n} + \mathbf{r}^N, t) - \hat{\tau}_N^+(\mathbf{n})P(\mathbf{n}, t)] \\ &\quad + [\hat{\tau}_N^+(\mathbf{n} - \mathbf{r}^N)P(\mathbf{n} - \mathbf{r}^N, t) - \hat{\tau}_N^-(\mathbf{n})P(\mathbf{n}, t)] \}, \end{aligned} \quad (3.8)$$

where N is the spatial dimension and $\mathbf{r}^N$ is the directional step size.

A continuum form of the above master equations can be obtained by using Taylor expansions about $\mathbf{n}$ and a *system size*[1] hypothesis to obtain a so-called Kramers-Moyal expansion, cf. [11], p266. That is, we arrive at the expansion

$$\partial_t P(\mathbf{n},t) = \sum_{N,k} \left\{ \frac{(\mathbf{r}^N \cdot \nabla)^k}{k!} [\hat{\tau}_N^-(\mathbf{n}) P(\mathbf{n},t)] + \frac{(-\mathbf{r}^N \cdot \nabla)^k}{k!} [\hat{\tau}_N^+(\mathbf{n}) P(\mathbf{n},t)] \right\} \tag{3.9}$$

and on truncating this to second order we obtain the Fokker-Planck equation

$$\partial_t P = -\sum_i \partial_i \left[A_i(\mathbf{x},t) P(\mathbf{x},t) \right] + \frac{1}{2} \sum_{i,j} \partial_i \partial_j \{ [B_{ij}(\mathbf{x}) P(\mathbf{x},t)] \}, \tag{3.10}$$

where

$$A_i(\mathbf{x}) = \sum_N r_i^N [\hat{\tau}_N^+ - \hat{\tau}_N^-]$$

and

$$B_{ij} = \sum_N r_i^N r_j^N [\hat{\tau}_N^+ + \hat{\tau}_N^-]$$

and in which we have replaced $\mathbf{n}$ by the more natural space variable $\mathbf{x}$. With B_{ij} identified as the ij-element of $\mathbf{B}(\mathbf{x},t)\mathbf{B}^T(\mathbf{x},t)$ we see that the Fokker-Planck equations (2.7) and (3.10) are equivalent.

The angiogenesis model we develop here is based on an idea due to Hill and Häder [14] who used a circular random walk model to simulate the trajectories of swimming micro-organisms. Here each tip cell is characterised by its speed, $s(t)$, and direction of motion, $\theta(t)$. By considering the direction of motion to be independent of the speed, an individual cell can be thought of as performing a random walk on the unit circle, described by the random variable, $\Theta(t)$, whose value is denoted by $\theta(t)$. At each time step of fixed length, k, the cell has a probability, $a(\theta(t))$, of turning clockwise through an angle δ, a probability, $b(\theta(t))$, of turning anti-clockwise through an angle δ, and a probability, $1 - a(\theta(t)) - b(\theta(t))$ of continuing in the same direction, for some functions $a(\theta(t))$ and $b(\theta(t))$.

[1] In one space dimension this is a *scaling assumption*. That is, there is a parameter δ such that the average step size and the variance of the step size are proportional to δ and such that the jump probabilities increase as δ becomes small. See [26, 23] for a full account of this both in the general case of reinforced random walks and in application to angiogenesis.

This can be written as

$$\begin{aligned} P(\Theta(t+k)-\Theta(t)=\delta) &= a(\theta(t)), \\ P(\Theta(t+k)-\Theta(t)=-\delta) &= b(\theta(t)), \\ P(\Theta(t+k)-\Theta(t)=0) &= 1-a(\theta(t))-b(\theta(t)). \end{aligned}$$

The probability density function f, for $\Theta(t)$, is defined by:

$$f(\theta,t)d\theta = P(\theta \leq \Theta(t) < \theta + d\theta).$$

In the limit as $k \to 0, \delta \to 0$, with $\frac{\delta^2}{k} < \infty$, it can be shown that f satisfies the Fokker-Planck equation:

$$\frac{\partial f}{\partial t} = -\frac{\partial}{\partial \theta}(\mu(\theta)f) + \frac{1}{2}\frac{\partial^2}{\partial \theta^2}(\sigma^2(\theta)f), \tag{3.11}$$

where

$$\begin{aligned} \mu(\theta) &= \lim_{k\to 0,\delta\to 0}\left(\frac{1}{k}E(\Theta(t+k)-\Theta(t))\right), \\ \sigma^2(\theta) &= \lim_{k\to 0,\delta\to 0}\left(\frac{1}{k}Var(\Theta(t+k)-\Theta(t))\right) \end{aligned}$$

and $E(X)$ and $Var(X)$ denote the expectation and variance of the random variable X. We now write (3.11) in the form

$$\frac{\partial f}{\partial t} = \frac{\partial}{\partial \theta}\left(D(\theta)f\frac{\partial}{\partial \theta}\left(ln\frac{f}{\tau(\theta)}\right)\right), \tag{3.12}$$

where we have the identification

$$\begin{aligned} D(\theta) &= \frac{\sigma^2(\theta)}{2}, \\ \tau(\theta) &= \frac{1}{\sigma^2(\theta)}exp\left(2\int\frac{\mu(\theta)}{\sigma^2(\theta)}d\theta\right). \end{aligned} \tag{3.13}$$

Equation (3.12) is the continuum limit of the reinforced random walk equation, see for example [26, 17],

$$\partial_t f_n = \hat{\tau}^+_{n-1}f_{n-1} + \hat{\tau}^-_{n+1}f_{n+1} - (\hat{\tau}^+_n + \hat{\tau}^-_n)f_n, \tag{3.14}$$

where $f_n(t) = f(n\delta, t)$.

If $D(\theta) = D$ constant, the transition rates, $\hat{\tau}_n^{\pm}$, are given by the normalised barrier model

$$\hat{\tau}_n^{\pm} = 2\lambda \frac{\tau((n \pm \frac{1}{2})\delta)}{\tau((n + \frac{1}{2})\delta) + \tau((n - \frac{1}{2})\delta)} \tag{3.15}$$

where $\lambda\delta^2 = D$. The time spent at $\theta = n\delta$ before turning is $\frac{1}{2\lambda}$, independent of n.

If $D(\theta)$ is not constant, the transition rates may be written as

$$\hat{\tau}_n^{\pm} = 2\bar{\lambda} \frac{\lambda((n \pm \frac{1}{2})\delta)\tau((n \pm \frac{1}{2})\delta)}{\tau((n + \frac{1}{2})\delta) + \tau((n - \frac{1}{2})\delta)} \tag{3.16}$$

where $D(\theta) = \bar{\lambda}\delta^2\lambda(\theta)$. For details of these constructions and their implementation see [19, 23, 24, 27].

Remark The stochastic differential equation for the angular movement is

$$d\theta = \left(D(\theta)\frac{\tau_\theta}{\tau} + D_\theta \right) dt + 2D(\theta)dW(t). \tag{3.17}$$

In [24] simulations of neovascular structures based on circular reinforced random walks give very good correlations with both *in vitro* and *in vivo* observations.

4 Conservation of Mass Formulation

The mathematical model described here is a macroscopic model governing the evolution of endothelial cell density $p(\mathbf{x}, t)$ in response to growth factors, growth inhibitors, haptotaxis as well as diffusion in the tissue matrix. From the law of mass conservation we write

$$\frac{\partial p}{\partial t} + \nabla \cdot \mathbf{J}(\mathbf{x}, t) = 0, \tag{4.1}$$

where $\mathbf{J}(\mathbf{x}, t)$ is the flux due to diffusion, chemotaxis and haptotaxis. That is

$$\mathbf{J}(\mathbf{x}, t) = -D\nabla p + p\nabla\chi + p\nabla F, \tag{4.2}$$

where $\chi(\mathbf{x}, t)$ is the chemotaxis coefficient which depends on a variety of growth factors and growth inhibitors, including VEGF, and F is the haptotaxis coefficient which depends on the tissue matrix properties, in particular fibronectin.

On combining (4.1) and (4.2) we obtain

$$\frac{\partial p}{\partial t} = D\Delta p - \nabla \cdot (p\nabla\chi) - \nabla \cdot (p\nabla F). \tag{4.3}$$

This equation is precisely of the form (2.7) and forms the basis of angiogenesis modelling developed in [3] and [4]. In order to simulate neovascular growth these authors adopt an idea due to Anderson and Sleeman [1] whereby (4.3) is spatially discretised using the well known Crank-Nicolson method. The result is an equation which resembles the master equation (3.8) above. However the coefficients of the density terms P are not transition probabilities but are nevertheless treated as such. Simulations following this idea also give good agreement with experimental and *in vivo* observations and have been exploited considerably in the literature.

5 Angiogenesis Modelled as a Stochastic Differential System

The final model presented here returns to the original stochastic differential equation (2.1) and uses this to govern the movement of the tips of the angiogenic sprouts, whose positions will be denoted by $\mathbf{x}_s$.

The drift vectors and diffusion matrices for the system can be derived from the expressions given for the Fokker-Planck equation in Section 3. Each of the components of the multivariable Wiener process is treated independently, giving a one-dimensional Wiener process for each of the space dimensions. In the one-dimensional case the transition rates are defined to be

$$\hat{\tau}_n^{\pm} = 2\lambda \frac{\tau((n \pm \frac{1}{2})h)}{\tau((n + \frac{1}{2})h) + \tau((n - \frac{1}{2})h)} \tag{5.1}$$

in which h represents a spatial "step" and $\lambda h^2 = D$ is constant. Using this expression and Taylor series expansions of $\tau^{\pm}$ provides the drift vectors:

$$A_i(\mathbf{x}, t) \;=\; \sum_N r_i^N \left[\hat{\tau}_N^+ - \hat{\tau}_N^-\right] \;=\; \sum_N r_i^N \, 2\lambda \left[\frac{h\tau_{x_i} + O(h^2)}{2\tau + O(h^2)}\right]$$

$$\approx \quad \lambda h^2 \frac{\partial}{\partial x_i}(\ln\,\tau) \;=\; \sum_{k=1}^{N_{var}} D\,\frac{\partial}{\partial U_k}(\ln\,\tau)\,\frac{\partial U_k}{\partial x_i}\,, \tag{5.2}$$

N_{var} being the number of variables that the transition probabilities depend on. The r_i^N are the components of $\mathbf{r}^N$, vectors of length h in the direction associated with the N^{th} spatial variable. Similarly, the diffusion matrices can be derived using the assumption that

$$\hat{\tau}_N^+ + \hat{\tau}_N^- = 2\lambda\,, \tag{5.3}$$

which leads to

$$B_{ij} \;=\; \sum_N r_i^N r_j^N\,[\hat{\tau}_N^+ + \hat{\tau}_N^-] \;=\; 2\lambda h^2\,\delta_{ij} \;=\; 2D\,\delta_{ij}\,, \tag{5.4}$$

in which δ_{ij} is the standard Kronecker delta function. Since $2D = \sigma^2$, where σ is the standard deviation of the random variable underlying the diffusion process, the diffusion matrix for the stochastic differential equation is $\sigma\mathbf{I}$.

Now, assuming that $\tau = \prod_{k=1}^{N_{var}} \tau_k(U_k)$ (as in [23, 24]) gives

$$\mathbf{A}(\mathbf{x},t) = \sum_{k=1}^{N_{var}} D\,\frac{\partial}{\partial U_k}(\ln\,\tau_k(U_k))\,\nabla U_k\,, \tag{5.5}$$

which leads to

$$d\mathbf{x}_s = \left[\sum_{k=1}^{N_{var}} D\,\frac{\partial}{\partial U_k}(\ln\,\tau_k(U_k))\,\nabla U_k\right] dt + \sigma\,d\mathbf{W}(t)\,. \tag{5.6}$$

The movement of each of the sprout tips is governed by an equation of this form.

The behaviour of this system will now be illustrated briefly using one two-dimensional and one three-dimensional test case. The movement of the sprout tips (and hence the transition probabilities) are assumed to depend on a chemotactic response to a tumour angiogenic factor, such as VEGF (denoted by $U_1 = V$), and a haptotactic response to fibronectin (denoted by $U_2 = F$). The transition probabilities are taken from [24] and given by $\tau = \tau_1(V)\tau_2(F)$, where

$$\tau_1(V) \;=\; \begin{cases} \exp\left(\frac{\chi_0 V}{D}\right) & p = 0 \\ (1+\gamma V)^{\frac{\chi_0}{\gamma D}} & p = 1 \\ \exp\left(-\frac{\chi_0}{\gamma D(p-1)(1+\gamma V)^{p-1}}\right) & p \neq 1 \end{cases} \tag{5.7}$$

$$\tau_2(F) \;=\; \exp\left(\frac{\rho_0 F}{D}\right). \tag{5.8}$$

The value of p can be adjusted to change the relative sensitivities of the movement to VEGF and fibronectin. The results shown below are for $p = 0$, which gives a constant response,

$$\chi_k(U_k) = D\,\frac{\partial}{\partial U_k}(\ln\,\tau_k(U_k))\,, \tag{5.9}$$

to both species. Following [24], the other parameter values are taken to be $\chi_0 = 2$, $\rho_0 = 0.25$ and $D = 0.00175$. Note that in the conservation of mass formulation of the previous section, this corresponds to taking

$$\mathbf{J}(\mathbf{x},t) = -D\,\nabla p + \sum_{k=1}^{N_{var}} p\,\chi_k(U_k)\,\nabla U_k\,. \tag{5.10}$$

A very simple algorithm, the stochastic Euler method [20], has been used to approximate the movement of the sprout tips. A time-step Δt is chosen, and for each sprout tip

$$\mathbf{x}^{n+1} = \mathbf{x}^n + \left[\sum_{k=1}^{N_{var}} \chi_k(U_k)\,\nabla U_k\right] dt + \sigma\,\widetilde{N}(0,\Delta t)\,, \tag{5.11}$$

where n is the time level and $\widetilde{N}(0,\Delta t)$ indicates a Gaussian distributed random variable with a mean of zero and variance Δt. This is the same approach as that used by Stokes and Lauffenburger [28, 29], though here the sprout tip position is updated directly, and the tip velocity is never explicitly calculated. In the numerical experiments below, the nondimensional time-step is taken to be 0.00125 and 1600 time-steps are carried out (giving a final time of $T = 2$).

The growth of the sprouts is augmented by two other processes.

- Anastomosis is carried out by projecting the sprout tip positions on to a background lattice of cells. If a tip enters a cell (or the immediate neighbour of a cell) which has previously been occupied by a sprout tip then tip-branch anastomosis is triggered. If two tips enter each other's neighbourhoods at the same time then tip-tip anastomosis occurs. The lattice used here has 500 cells in each spatial direction.

- Branching is implemented by checking each segment of each sprout tip's path, and checking whether a randomly generated number (with uniform distribution on $[0, 1]$) is less than $p_b \, \Delta r \, \Delta t$, where Δr is the length of the segment. If the random number is low enough then a branch is generated. The branching rate is taken here to be $p_b = 4$ [24].

The underlying reaction kinetics are assumed here to have reached a steady state and are represented by simple analytic profiles, designed to simulate a situation where there is a source of VEGF (the tumour) at one side of the domain. Future publications will describe how the movement of the sprout tips can be coupled with a simple model of the background chemistry (such as that presented in [19, 23]) but the results presented here will simply demonstrate the use of a stochastic differential equation model for the movement of the sprout tips.

The profiles chosen for VEGF and fibronectin are given by [24]

$$\begin{aligned} V(x,y) &= \begin{cases} V_0 \exp(-k_1 |\mathbf{x} - \mathbf{x}_t|) & |\mathbf{x} - \mathbf{x}_t| > r_t \\ V_0 \exp(-k_1 r_t) & \text{otherwise} \end{cases} \\ F(x,y) &= F_0 \exp(-k_2 y) \,, \end{aligned} \tag{5.12}$$

in which $\mathbf{x}_t$ denotes the position of the centre of the tumour and r_t its radius. The domain is a square (in 2D) or cube (in 3D) of side $[0, L]$. The profiles given in (5.12) are illustrated for the two-dimensional case in Figure 3. As in [24], the free parameters are chosen to be $k_1 = 1$, $k_2 = 2$ (nondimensionalisation removes dependence on V_0 and F_0), $r_t = 0.2$ and $\mathbf{x}_t = (0.5, 1)^T$ in two dimensions or $\mathbf{x}_t = (0.5, 1, 0.5)^T$ in three dimensions.

The two-dimensional test case is initialised at $T = 0$ with four sprouts, evenly spaced along $y = 0$. The paths of the sprout tips at $T = 0.5, 1, 1.5, 2$ are shown in Figure 4. The sprouts are clearly drawn towards the source of VEGF and branching and anastomosis are visible (the latter highlighted by small solid circles). It also shows that in this situation the sprouts accelerate towards the source of VEGF as they get closer to it (and the concentration of VEGF increases relative to that of fibronectin). Similar behaviour is also visible in the three-dimensional test case. This uses the same parameters but is initialised with four evenly spaced sprouts along the line defined by $x = z$, $y = 0$. Figure 5 shows the progress of the sprouts at times $T = 0.5, 1, 1.5, 2$. The notional surface of the tumour/source of VEGF is illustrated in each

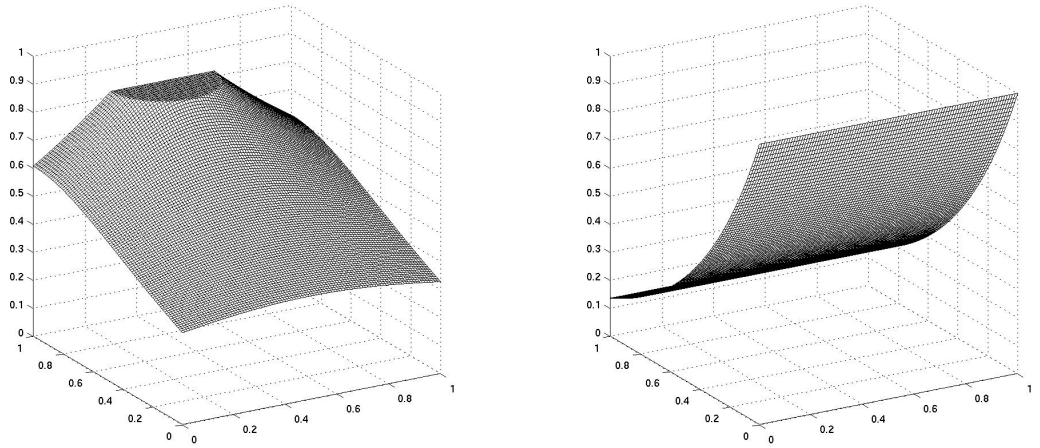

Figure 3: The steady state profiles for VEGF (left) and fibronectin (right) in two space dimensions.

figure. Note that the sprouts are programmed to stop when they reach the source.

6 Conclusions

Basing the mathematical modelling of angiogenesis on stochastic differential equations provides an underlying philosophy which unifies a number of current modelling techniques. These include the individual cell-based models using the theory of reinforced random walks, the macroscopic models based on conservation of mass leading to cell density models, as well as the hybrid methods based on numerical discretisation of cell density models.

The stochastic foundation is very general and may be used to explore other forms of angiogenesis beyond that of sprouting angiogenesis considered here. The ideas expressed in this paper are to be developed in future work to include the kinetic dynamics of VEGF, haptotaxis of fibronectin as well as proteolytic enzymes and the response to anti-angiogenic drugs. Additionally it is of importance to model the role of pericytes in stabilising the neovascular network as well as the incorporation of blood flow.

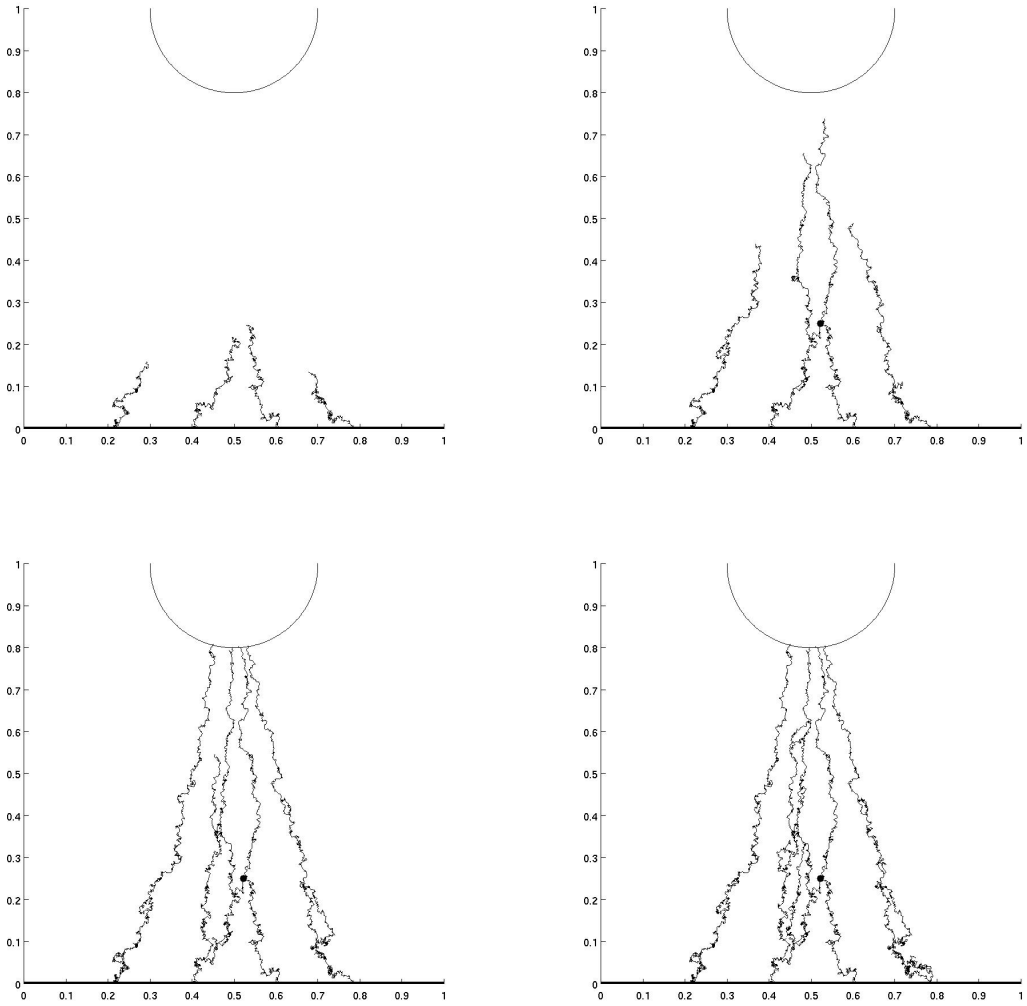

Figure 4: Snapshots of the growth of the angiogenic sprouts in two space dimensions at $T = 0.5, 1, 1.5, 2$.

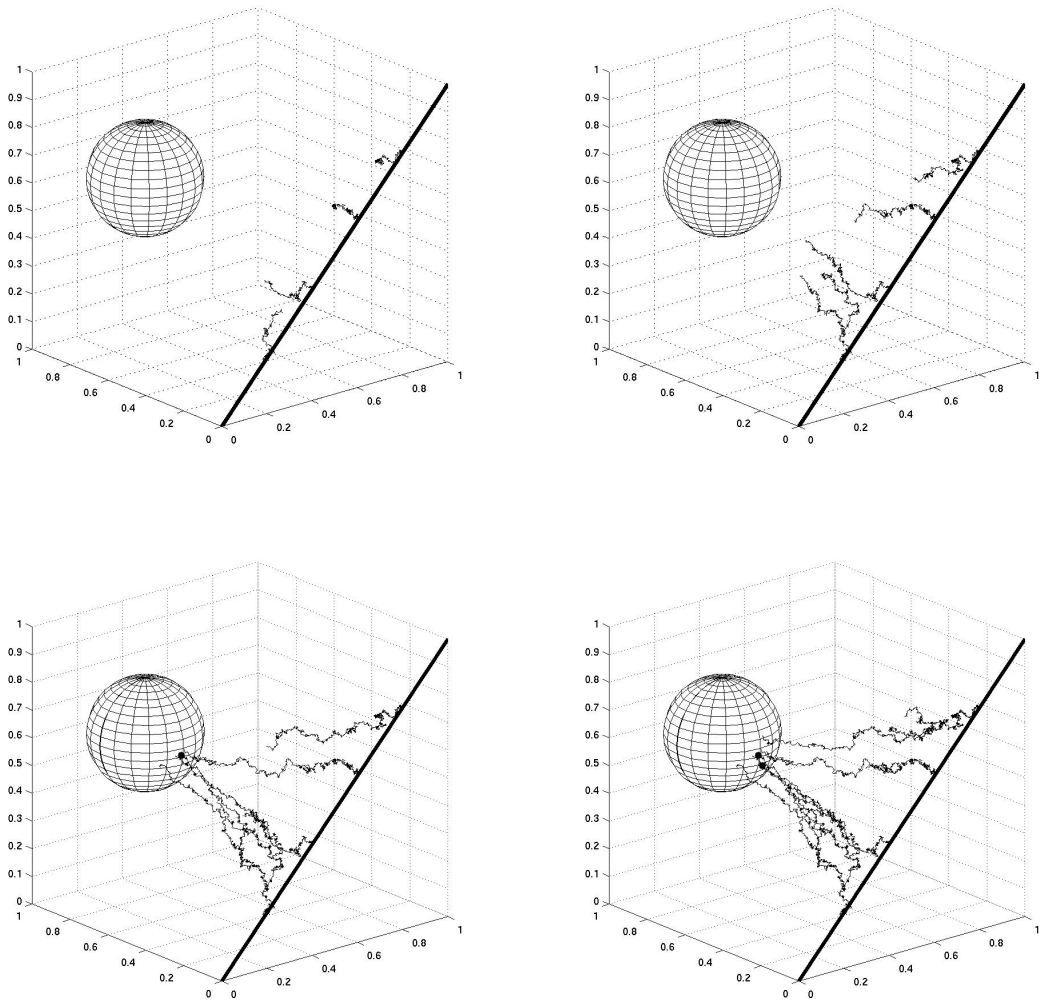

Figure 5: Snapshots of the growth of the angiogenic sprouts in three space dimensions at $T = 0.5, 1, 1.5, 2$.

References

[1] A.R.A.Anderson, B.D.Sleeman, I.M.Young, B.S.Griffiths and W.Robertson, Nematode movement along a gradient in a structurally heterogeneous environment II: Theory, Fundamental and Applied Nematology, **20**, 165-172, 1997.

[2] P.H.Burri, R.Hlushchuk and V.G.Djonov, Intussusceptive angiogenesis: Its emergence, its characteristics and its significance, Development Dynamics, **231**, 474-488, 2004.

[3] M.A.J.Chaplain and A.R.A.Anderson, Modelling the growth and form of capillary networks. In *On growth and form*, M.A.J.Chaplain, G.D.Singh and J.C.McLachlan (Eds). Wiley: New York, 225-249, 1999.

[4] M.A.J.Chaplain and A.M.Stuart, A model mechanism for the chemotactic response of endothelial cells to tumour angiogenesis factor, IMA J. Math. Appl. Med. Biol., **10**, 149-168, 1993.

[5] P.Carmeliet and R.Jain, Angiogenesis in Cancer and other Diseases, Nature, **407**, 249-257, 2000.

[6] N.Ferrara, H.P.Gerber, J.LeCouter, The Biology of VEGF and its Receptors, Nat. Med., **9**, 669-676, 2003.

[7] R.Folberg and A.J.Maniotis, Vasculogenic mimicry, APMIS, **112**, 508-525, 2004.

[8] J.Folkman, Role of Angiogenesis in Tumour Growth and Metastasis, Semin. Oncol., **29**, 15-18, 2002.

[9] J.Folkman, Angiogenesis, Ann. Rev. Med., **57**, 1-18, 2006.

[10] D.Fukumura and R.K.Jain, Imaging angiogenesis and the microenvironment, APMIS, **116**, 695-715, 2008.

[11] C.W.Gardiner, *Handbook of Stochastic Methods*, Springer-Verlag, 1983.

[12] S.J.Harper and D.O.Bates, VEGF-A splicing: the key to anti-angiogenic therapeutics? Nat. Rev. Cancer, **8**, 880-887, 2008.

[13] B.Heissig, K.Hattori, S.Dias, M.Friedrich, B.Ferris, N.R.Hackett, et al., Recruitment of Stem and Progenitor Cells from the Bone Marrow Niche requires MMP-9 mediated release of Kit-ligand, Cell, **109**, 625-637, 2002.

[14] N.A.Hill and D.P.Häder, A Biased Random Walk Model for the Trajectories of Swimming Micro-organisms, J. Theor. Biol., **186**, 503-526, 1997.

[15] F.Hillen and A.W.Griffioen, Tumour vascularization: Sprouting angiogenesis and beyond, Cancer Metastasis Rev., **26**, 489-502, 2007.

[16] J.Holash, P.C.Maisonpierre, D.Compton, P.Boland, C.R.Alexander, D.Zagzag, et al., Vessel Cooption, Regression and Growth in Tumors mediated by Angiopoietins and VEGF, Science, **284**, 1994-1998, 1999.

[17] H.A.Levine, B.D.Sleeman, A System of Reaction Diffusion Equations arising in the Theory of Reinforced Random Walks, SIAM J. Appl. Math., **57**, 683-730, 1997.

[18] H.A.Levine, B.D.Sleeman and M.Nilsen-Hamilton, Mathematical Modelling of the onset of Capillary formation initiating Angiogenesis, J. Math. Biol., **42**, 195-238, 2001.

[19] H.A.Levine, S.Pamuk, B.D.Sleeman and M.Nilsen-Hamilton, A Mathematical Model of Capillary Formation and Development in Tumour Angiogenesis: Penetration into the Stroma, Bull. Math. Biol., **63**, 801-863, 2001.

[20] G.N.Mil'shtein, Approximate integration of stochastic differential equations, Theory Prob. Appl., **19**, 557-562, 1974.

[21] S.Patan, Vasculogenesis and Angiogenesis, Cancer Treat. Res., **117**, 3-32, 2004.

[22] M.S.Pepper and M.Skobe, Lymphatic endothelium: Morphological, molecular and functional properties, Journal of Cell Biology, **163**, 209-213, 2003.

[23] M.J.Plank and B.D.Sleeman, A Reinforced Random Walk Model of Tumour Angiogenesis and Anti-Angiogenic Strategies, IMA J. Math. Med. Biol., **20**, 135-181, 2003.

[24] M.J.Plank and B.D.Sleeman, Lattice and Non-Lattice Models of Tumour Angiogenesis, Bull. Math. Biol., **66**, 1785-1819, 2003.

[25] W.Risau, Mechanisms of Angiogenesis, Nature, **386**, 671-674, 1997.

[26] H.G.Othmer and A.Stevens, Aggregation, Blow-up and Collapse: the ABC's of Taxis in Reinforced Random Walks, SIAM J. Appl. Math., **57**, 1044-1081, 1997.

[27] B.D.Sleeman and I.P.Wallis, Tumour Induced Angiogenesis as a Reinforced Random Walk: Modelling Capillary Network Formation without Endothelial Cell Proliferation, J. Math. Comp. Modelling, **36**, 339-358, 2002.

[28] C.L.Stokes and D.A.Lauffenberger, Analysis of the Roles of Microvessel Endothelial Cell Random Motility and Chemotaxis in Angiogenesis, J. Theor. Biol., **152**, 377-403, 1991.

[29] C.L.Stokes, D.A.Lauffenberger and S.K.Williams, Migration of Individual Microvessel Endothelial Cells: Stochastic Model and Parameter Measurement, J. Cell. Sci., **99**, 419-430, 1991.